Structures and Energetics of Adenosine Radicals: (2′-dAdo − H)•

Francesco A. Evangelista[†] and Henry F. Schaefer III*[,‡]

Scuola Normale Superiore di Pisa, 56126 Pisa, Italy, and Center for Computational Chemistry, University of Georgia, Athens, Georgia 30602-2525

Received: May 18, 2004

The radicals and anions generated from the 2′-deoxyriboadenosine molecule were studied using the carefully calibrated computational scheme described in *Chem. Rev.* **2002**, *102*, 231. The method employs three different density functionals in connection with a double-ζ plus polarization and diffuse functions, DZP++, basis set. For all species considered, the optimized geometries, energies, and second derivatives were obtained. The adiabatic electron affinities (AEAs), vertical electron affinities (VEAs), and vertical detachment energies (VDEs) were determined. The nature of the radicals and anions was investigated, analyzing, respectively, the spin densities and the highest occupied molecular orbitals. Natural population analysis was applied to examine the electron distributions. Prediction of substantial positive AEAs in the range of 0.99−3.47 eV was supported by the analysis of the VEAs (0.08−2.44 eV) to correlate geometry perturbations with the AEA values. Vertical detachment energies are in the range of 1.78−3.65 eV. The energetic order found for the radicals is C(aliphatic) < N(amino) < O(hydroxyl) < C(aromatic). The radical created at $C_{1'}$ was found to be the most stable, due to delocalization of the unpaired electron on the adenine moiety. The anion energies follow the trend N(amino) < O(hydroxyl) < C(aliphatic) < C(aromatic). Four of the five aliphatic anions are subject to dissociative behavior. This finding has several biological implications and may explain the possible degrees of damage to the DNA double strand.

1. Introduction

There is broad scientific interest in the replication, translation, and transduction of genetic information stored in DNA. A major, but less understood, problem is the chemistry of DNA damage and how this is reflected in the living cell metabolism.[1] Damages to the genetic information and strand breaks in the structure may be caused by different factors, for example, reaction with chemical species or interaction with highly energetic photons and electrons. These sources of damage have been investigated experimentally on both DNA and some model systems involving radicals,[2−7] photons,[8−10] and electrons.[11−14] Some of these sources of damage are correlated among themselves. For example, irradiation of a water containing medium will produce hydroxyl radicals and also electrons. This makes the problem more complex, as different effects must be taken into consideration.

Comprehension of the mechanisms underlying these experimental observations requires the chemistry of the basic components to be known. DNA is commonly viewed as a polymer of nucleotides. Each nucleotide is composed of a phoshate group linked to a 2′-deoxyribose ring, which is in turn linked at the $C_{1'}$ position to a purinic or pyrimidinic base.

Many theoretical and experimental studies have elucidated the chemistry of the nucleic acid components. The free nucleic acid bases have been studied by different authors from both the experimental[11,15−21] and theoretical[22−26] points of view. Several theoretical investigations of the isolated adenine radicals and anions have been conducted to determine the energetic ordering and to predict the electron affinities.[22,27−29] The adenine−thymine base pair has been investigated by means of both semiempirical and DFT methods.[25,26] Concerning the sugar ring, several authors have investigated ribose, 2′-deoxyribose, and their radicals at Hartree−Fock and correlated levels of theory, but no work on the anionic states is known.[30−33]

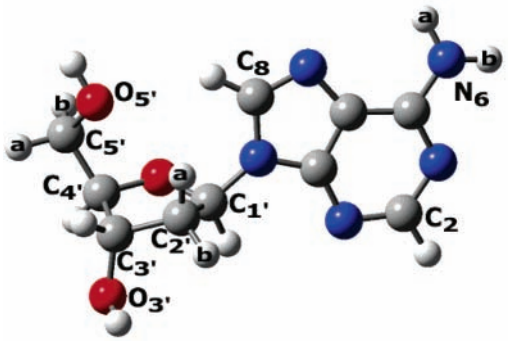

Figure 1. Numbering scheme of 2′-deoxyadenosine. The atoms are indicated with the following colors: C gray, H white, N blue, and O red. The letters a and b are used to distinguish between hydrogens linked to the same atom.

A number of aspects of the adenine nucleoside and nucleotide have already been studied: the crystal structure,[34−36] the gas phase structure obtained by ion mobility methods,[37] the chemistry of two radicals derived from adenosine,[5,6] and a general theoretical study of the nucleoside radical anions by Richardson and co-workers.[38]

The aim of the present research is to contribute to the understanding of the chemistry of the basic components of DNA by investigating the radicals produced from 2′-deoxyadenosine (2′-dAdo) by removing one hydrogen atom. The structure and numbering scheme of 2′-dAdo used in this article are depicted in Figure 1. In this paper we adopt the standard nomenclature used in Saenger's *Principles of Nucleic Acid Structure*.[39] With Figure 1 in view, it should be noted that adenosine radicals are

* Corresponding author E-mail address: hfs@uga.edu.
† Scuola Normale Superiore di Pisa.
‡ University of Georgia.

10.1021/jp040361r CCC: $27.50 © 2004 American Chemical Society
Published on Web 10/26/2004

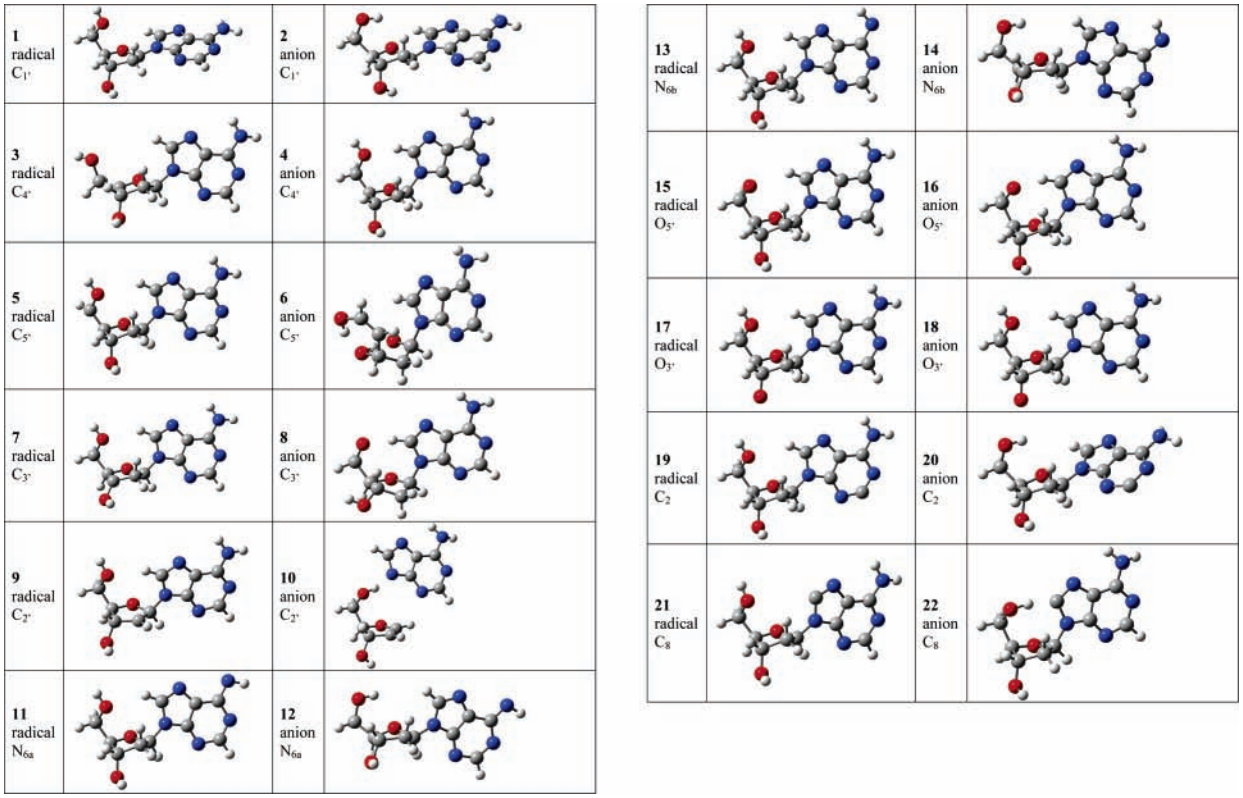

Figure 2. Qualitative structures of the radicals and anions optimized with the B3LYP/DZP++ method.

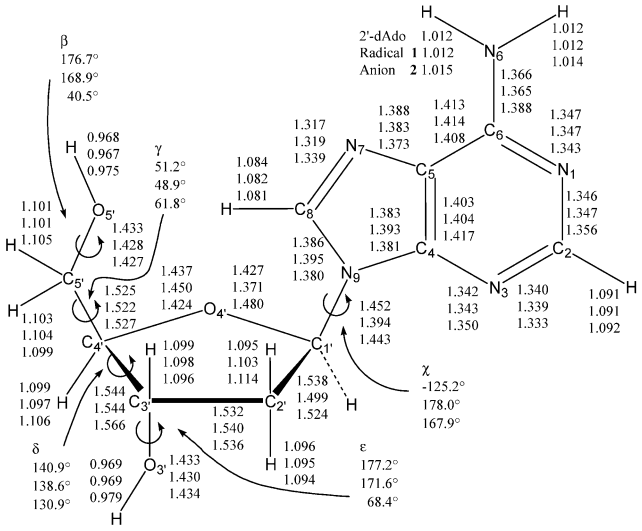

Figure 3. Bond lengths and major dihedral angles in the closed-shell neutral 2′-dAdo, radical **1**, and the closed-shell anion **2**, predicted at the B3LYP/DZP++ level.

also involved in vitamin B12 reactions, but with no OH group attached to atom $C_{5'}$.

2. Theoretical Methods

Several general considerations may be addressed concerning the adenosine structure. The conformational spaces of the nucleosides and nucleotides are considerably complex,[37,40] and different ways of solving the problem of finding the lowest energy conformation may be formulated. In a typical conformational search, one selects a certain number of starting structures, representative of the conformational space, and optimizes them. One might set up a conformational search that will generate twelve different values for each dihedral angle, with a spacing of 30°, and two conformations for each ribose ring. For 2′-deoxydenosine, there are four major dihedral angles (β, γ, ϵ, and χ) and one ribose ring (Figure 3). The starting number of conformations to be considered is huge, 41 472. The application of conformational searches to nucleosides, and a fortiori to nucleotides, is challenging.

In this research, we face the conformational problem in a much more intuitive manner. Since the B DNA form is considered the most important one for biological systems,[41] we optimized the 2′-dAdo molecule starting from a conformation identical to B DNA, where the phosphorus atoms connected to $O_{3'}$ and $O_{5'}$ were substituted by hydrogen atoms.

Energies, optimized structures, vibrational frequencies, and spin densities were determined using three generalized gradient approximation (GGA) exchange-correlation functionals: B3LYP, BLYP, and BP86. These are combinations of Becke's exchange functionals [the three-parameter HF/DFT hybrid exchange functional (B3)[42] or the pure exchange functional (B)[43]] with the dynamical correlation functional of Lee et al. (LYP)[44] or that of Perdew (P86).[45,46]

All computations were performed using double-ζ quality basis sets with polarization and diffuse functions, DZP++. The DZP++ basis sets were constructed by augmenting the Huzinage−Dunning[47,48] sets of contracted double-ζ Gaussian functions with one set of p-type polarization functions for each H atom and one set of five d-type polarization functions for each C, N, and O atom ($\alpha_p(H) = 0.75$, $\alpha_d(C) = 0.75$, $\alpha_d(N) = 0.80$, and $\alpha_d(O) = 0.85$). To complete the DZP++ basis, one even-tempered s diffuse function was added to each H atom, while even-tempered s and p diffuse functions were centered on each heavy atom. The even-tempered orbital exponents were determined according to the prescription of Lee and Schaefer:[49]

$$\alpha_{\text{diffuse}} = \frac{1}{2}\left(\frac{\alpha_1}{\alpha_2} + \frac{\alpha_2}{\alpha_3}\right)\alpha_1$$

where α_1, α_2, and α_3 are the three smallest Gaussian orbital

exponents of the s- or p-type primitive functions for a given atom ($\alpha_1 < \alpha_2 < \alpha_3$). The final DZP++ set contains 6 functions per H atom (5s1p/3s1p) and 19 functions per C, N, or O atom (10s6p1d/5s3p1d), yielding a total of 420 contracted functions for the adenosine molecule and 414 for the adenosine radicals and anions.

This DZP++ basis set has been used in systematic calibrative EA studies[50] on a wide range of molecules. These combinations of functionals and basis set have been shown to predict electron affinities with average errors less than 0.12 eV in the case of a closed-shell anion and the corresponding open-shell neutral. An unrestricted version of DFT was used for the radicals and the restricted form for the anions. All structures were optimized using analytic gradients with tight convergence criteria. Numerical integrations were performed using the GAUSSIAN 94[51] default grid consisting of 75 radial shells with 302 angular points per shell. Vibrational frequency evaluations were done on all radicals and on all the stable anion structures; no scaling factor was applied.

Adiabatic electron affinities were computed as the difference between the absolute energies of the appropriate neutral and anion species at their respective optimized geometries

$$\mathrm{AEA} = E_{\mathrm{neut}} - E_{\mathrm{anion}}$$

The vertical electron affinities were computed as the energy difference between the neutral species and the anion species, both at the optimized neutral geometry

$$\mathrm{VEA} = E_{\mathrm{neut\ (neut\ opt)}} - E_{\mathrm{anion\ (neut\ opt)}}$$

The vertical detachment energies were computed as the energy difference between the neutral species and the anion species, both at the optimized anion geometry

$$\mathrm{VDE} = E_{\mathrm{neut\ (anion\ opt)}} - E_{\mathrm{anion\ (anion\ opt)}}$$

For all of the radicals, plots of the total spin density were computed. This quantity is given in standard DFT methods by the difference between the density of α and β electrons:

$$\rho^{s}(\mathrm{r}) = \rho^{\alpha}(\mathrm{r}) - \rho^{\beta}(\mathrm{r})$$

The total spin density allows us examine the extent of delocalization of the unpaired electron within the molecular framework. For the anions, the HOMOs were computed at the B3LYP/DZP++ level and plotted. Natural population atomic (NPA) charges were determined using the B3LYP functional and the DZP++ basis set with the natural bond order (NBO) analysis of Reed and Weinhold.[52−55]

This paper is a contribution to the chemical physics of biomolecules in the gas phase. For two reasons, we have not considered solvent effects. The first is practical: the consideration of solvent effects by continuum models would necessarily degrade the theoretical results. Second, we hold the view that the deepest understanding of biochemistry will emerge when the gas phase systems have first been reliably characterized. When this approach is combined with microsolvation studies (not currently possible with more than a few solvent molecules), a comprehensive understanding should emerge.

3. Results

Optimization of 2′-dAdo in the B DNA conformation (as explained in the Introduction) resulted in a structure that is in good agreement with the average B DNA parameters: the ribose ring having a $C_{2'}$-*endo* conformation and the purine group in the anti arrangement, while the base has a flat structure except for the amino group hydrogens that are not coplanar with respect to the two adenine rings. The N−C glycosyl bond length is 1.452 Å, compared to the experimental crystallographic value found for 2′-deoxyadenosine monohydrate,[34] 1.472 Å. The largest deviation in the dihedral angles is observed for β ($H_{5'}-O_{5'}-C_{5'}-C_{4'}$), which has a theoretical value of 177 versus 214° in B DNA.[56] Here, it is important to consider that in DNA the values of the structural parameters are strongly dependent on the neighborhood of the nucleotide and that, locally, large deviations from the average values are observed. This candidate structure was used to generate all the radicals and anions considered in the present investigation. The total energy at the B3LYP/DZP++ level for this conformation is −888.504 30 Hartree.

TABLE 1: Total and Relative Energies of the Radicals Derived from Adenosine (in kcal/mol)

		B3LYP		BLYP		BP86	
structure		relative	relative + ZPVE	relative	relative + ZPVE	relative	relative + ZPVE
1	$C_{1'}$	0.0	0.0	0.0	0.0	0.0	0.0
3	$C_{4'}$	2.0	1.9	1.6	1.5	2.2	2.0
5	$C_{5'}$	3.8	3.9	4.6	4.8	4.6	4.8
7	$C_{3'}$	4.4	4.6	5.3	5.7	5.3	5.6
9	$C_{2'}$	9.3	8.7	10.4	9.8	10.6	10.3
11	N_{6a}	10.1	10.2	9.8	10.1	11.4	11.6
13	N_{6b}	11.0	11.1	10.8	11.1	12.3	12.5
15	$O_{5'}$	12.1	11.9	10.5	10.5	11.3	11.2
17	$O_{3'}$	11.7	12.0	12.2	12.3	13.3	13.4
19	C_2	17.6	18.2	18.8	19.5	18.8	19.5
21	C_8	25.8	26.1	26.2	26.2	24.0	24.7

Starting from an A DNA conformation, we obtained a final optimized structure with $C_{3'}$-*endo* conformation at the sugar ring. This form was found to be less stable with respect to the $C_{2'}$-*endo*, the energy difference being very small, less than 0.3 kcal/mol. The starting structures for the radicals were thus obtained by removing one hydrogen atom from the $C_{2'}$-*endo* 2′-dAdo molecule. The anion structures were obtained starting from the optimized radical geometries.

3.1. Geometry and Energetics. *3.1.1. 2′-dAdo Radicals.* The optimized structures of the radicals and anions computed at the B3LYP/DZP++ level are sketched in Figure 2. The total and relative energies of the radicals are reported in Table 1. The numbering scheme adopted is such that the radicals are ordered with increasing energy computed at the B3LYP/DZP++ level, and each radical structure is followed by its anion. The 2′-dAdo molecule contains 13 hydrogen atoms, but only 11 of the possible radicals have unique structures. This is because there are two carbon centers, $C_{3'}$ and $C_{5'}$, each having two hydrogen atoms that are equivalent when abstracted and the structure is optimized. The radicals obtained by rearrangement of the 11 radicals considered here are not investigated, except for the previously studied[6] (5′*R*)-5′,8-cyclo-2′-deoxy-7-adeonosyl radical. This has an energy of −887.858 75 hartree, compared to the energy of **1**, −887.850 34 hartree. Thus, the former structure lies 5.3 kcal/mol lower in energy.

The radical energies are spread over a range of 26 kcal/mol. The three functionals used predict minor differences in the energetic order; the following analysis is based on the B3LYP functional results. The radicals produced at aliphatic centers are more stable with respect to those produced on heteroatoms (N and O) and on aromatic C; the observed energetic trend for the radicals is

$$\mathrm{C(aliphatic)} < \mathrm{N(amino)} < \mathrm{O(hydroxyl)} < \mathrm{C(aromatic)}$$

The geometry of the aliphatic radicals generally differs substantially from that of the closed-shell neutral 2′-dAdo only around the radical center. The carbon center goes from a tetrahedral sp^3 hybridization to a planar or almost planar sp^2 hybridization. This causes planarity at the radical center, resulting in an almost flat radical **9** and an intermediate geometry for the other aliphatic radicals. The conformation of the ribose ring is $C_{2'}$-*endo* for all the species except for the flat ring radical **9**. Significant distortions are observed for radical **3**, in which case planarity leads to a more "open" structure, and this can be seen from the distance between C_8 and $O_{5'}$, which is a measure of the distance of the nucleic acid base with respect to the backbone phosphate chain. The deviation is large considering that in 2′-dAdo the distance $C_8-O_{5'}$ is 3.6 Å while in radical **3** the value increases to 5.0 Å.

The conformation of the adenine group with respect to the ribose ring, measured by the dihedral angle χ ($O_{4'}-C_{1'}-N_9-C_4$), experiences an exception in radical **1**. Detailed structure information for radical **1** and anion **2** is presented in Figure 3. Generally, in B DNA an anti conformation is found, with $\chi \sim -100°$; in 2′-dAdo this angle is equal to $-125.2°$. For radical **1**, we found that the adenine framework is rotated and $\chi = 178°$. The dihedrals pertaining to the backbone (β, γ, ϵ) do not differ from the values found in 2′-dAdo. Relevant geometric distortions are observed in the proximity of the radical center; in particular, the bond with atoms $C_{2'}$, $O_{4'}$, and N_9 shorten by 0.04−0.06 Å. The five member ring of the adenine framework is also affected, in particular the two bonds N_9-C_8 and N_9-C_4.

For the aliphatic radicals the observed stability order is

$$1' (\mathbf{1}) > 4' (\mathbf{3}) > 5' (\mathbf{5}) > 3' (\mathbf{7}) > 2' (\mathbf{9})$$

which differs from the order computed for thymidine 3′,5′-diphosphoric acid radicals studied at the ROB3LYP/6-31G*//ROB3LYP/3-21G* level.[57] For the latter molecules the order found is

$$4' (\mathbf{3}) > 5' (\mathbf{5}) > 1' (\mathbf{1}) > 3' (\mathbf{7}) > 2' (\mathbf{9})$$

The torsion motion involving the dihedral angle χ and the high stability of radical **1** are both features that are not observed for the thymine derivative but are possible for 2′-dAdo, since the unpaired electron in the p orbital of $C_{1'}$ can undergo conjugation with the adenine framework. Delocalization of the unpaired electron will lower the energy of the system, such an argument being based on the particle-in-a-box model. All this can happen only if the glycosyl link undergoes a torsional motion and the p orbital of $C_{1'}$ is in phase with the π cloud of the adenine molecule. This is not possible in the thymine derivative, probably because there is no extensive delocalization of the unpaired electron on the pyrimidine ring.

The latter result is quite interesting, since in DNA the rotation about the glycosidic bond will break the coplanarity of the two nucleic acid bases in the base pair. The loss of coplanarity results in the break of two hydrogen bonds of the base pair and thus in a strand opening.

The energy of radical **1** at the geometry of the $C_{2'}$-*endo* 2′-dAdo (with the constraint $\chi = -125°$ as found for 2′-dAdo) is predicted to be higher by 3.6 kcal/mol, this being the lowering in energy when the conformation changes from the B DNA-like to the rotated radical minimum. If this additional stabilization was not possible, the energetic order would probably agree with the one obtained for the thymine derivative.

The base pairing energy of adenine with thymine, A + T → AT, is estimated by Richardson[25] at the B3LYP/DZP++ level (without ZPVE correction) to be −13.8 kcal/mol. The experimental value[58] obtained by means of field-ionization mass spectroscopy is −13.0 kcal/mol.

Suppose we pair the 2′-dAdo nucleoside to thymine and generate radical **1** by hydrogen abstraction; a raw estimated energy difference between the unrotated paired structure and the rotated nonpaired structure is 10.2 kcal/mol, with the paired structure being the more stable. This means that in this model the base is not able to rotate along the glycosyl link easily because of the ca. 10 kcal/mol barrier. In DNA, we have to consider additional constraints, and this will probably exclude completely the rotation that we are considering.

The rationalization of the stability order of the other four radicals is based on the simply established fact that the radicals **3**, **5**, and **7** have an oxygen atom in an α position that can give conjugation while the less stable **9** does not.[30] Radicals **5** and **7** are interesting, since they involve atoms that are essential for the DNA strand integrity. For both those species, the bond length between the radical center and the neighbor atoms decreases.

The radicals produced on heteroatoms and on aromatic carbons are higher in energy with respect to **1** by more that 10 kcal/mol. The isolated *adenine* radical energetics were investigated in a previous paper,[29] and the following order was found (B3LYP/DZP++ with ZPVE):

11 (0.00 kcal/mol) < **13** (1.07 kcal/mol) < **19** (7.18 kcal/mol) < **21** (14.84 kcal/mol)

This compares with the 2′-dAdo results (B3LYP/DZP++ with ZPVE):

11 (0.00 kcal/mol) < **13** (0.90 kcal/mol) < **19** (7.95 kcal/mol) < **21** (15.85 kcal/mol)

It is seen that the results do not change substantially in going from the nucleic acid base to the nucleoside. This would suggest that similar results may be found for the nucleotides. Extending those results to the base pair is not possible since hydrogen bonding interactions with the counter base can have a significant influence on the energetics, depending on which radical is considered.

Geometrical changes for the radicals produced on heteroatoms and on aromatic carbons are less pronounced with respect to the aliphatic radicals. All the structures have a $C_{2'}$-*endo* conformation at the ribose ring. Radicals **11** and **13** created at the amino group nitrogen N_6 have the remaining hydrogen atom coplanar to the adenine framework. The other radical structures do not exhibit this feature. Details of the structure of radical **11** are given in Figure 4. The major dihedral angles show very small difference with respect to 2′-dAdo, thus indicating that the ribose ring is unaffected by radical production; this is also confirmed by the bond lengths which have similar values to the closed-shell neutral molecule. The glycosil link is also unaffected. Substantial changes in the bond lengths of the adenine part are observed and interpreted as an effect of delocalization of the unpaired electron on the π cloud.

Radicals **15** and **17** are both created at oxygen atoms. The structure for radical **15** is depicted in Figure 5. For **15** the $C_{5'}-C_{4'}$ bond length increases (1.52 Å → 1.60 Å) while the $C_{5'}-O_{5'}$ bond length decreases (1.42 Å → 1.35 Å) with respect to 2′-dAdo. In this case, the other variations in the geometry are observed near the radical center, the dihedral angles show minor differences, and the adenine framework is essentially unaffected. A similar result is found for **17**: the $C_{3'}-C_{4'}$ bond length increases (1.54 Å → 1.60 Å) and the $C_{3'}-O_{3'}$ distance decreases

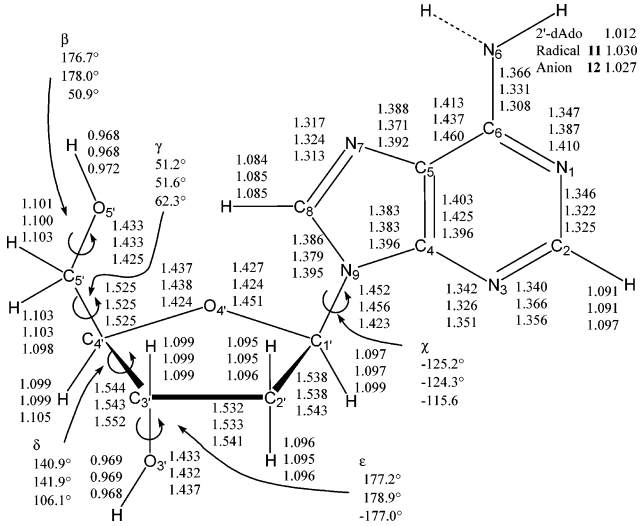

Figure 4. Bond lengths and major dihedral angles in the closed-shell neutral 2′-dAdo, radical **11**, and the closed-shell anion **12**, predicted at the B3LYP/DZP++ level.

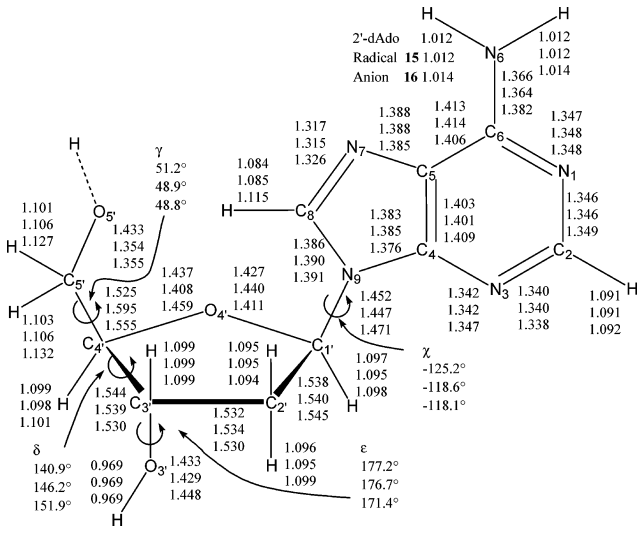

Figure 5. Bond lengths and major dihedral angles in the closed-shell neutral 2′-dAdo, radical **15**, and the closed-shell anion **16**, predicted at the B3LYP/DZP++ level.

(1.43 Å → 1.37 Å). Radicals **15** and **17** cannot be formed in DNA, since the oxygen atoms are part of the phosphate groups.

Abstracting a hydrogen atom from the two aromatic carbon atoms results in only small geometry distortions with respect to 2′-dAdo; major geometrical relaxations are observed in the adenine framework and are localized near the radical center. In radical **21**, one effect is the "opening" of the molecule that can be underlined by considering the $C_8-O_{5'}$ distance increase with respect to 2′-dAdo, 3.60 Å → 3.95 Å. This might be caused by the loss of hydrogen H_8, which can interact in 2′-dAdo with $O_{5'}$.

3.1.2. 2′-dAdo Anions. The total and relative energies of the anions are listed in Table 2. The anions generated from the radicals adding an extra electron may be divided into two categories. In the first category, we have all those species that preserve the connectivity of the original radicals, showing only discrete geometrical distortions with respect to the starting structure. In the second category, we put all those anions that have a different connectivity with respect to the analogous radical and show drastic geometrical changes. In the second category, we observe a dissociation of one, or more than one, bond. Clearly this classification has some problems with intermediate situations, but in our case it can be applied without misgivings. From the experimental point of view, this means that for certain radicals the AEA cannot be determined by means of techniques that rely on the formation of a stable anion, for example as required in photoelectron spectroscopy experiments.[50]

TABLE 2: Relative Energies of the Stable Anions Derived from Adenosine (in kcal/mol)

		B3LYP		BLYP		BP86	
structure		relative	relative + ZPVE	relative	relative + ZPVE	relative	relative + ZPVE
16	$O_{5'}$	0.0	0.0	0.0	0.0	0.0	0.0
12	N_{6a}	0.7	1.6	0.9	1.9	1.6	2.8
14	N_{6b}	1.2	2.2	1.5	2.5	2.1	3.4
22	C_8	5.0	5.0	*a*	*a*	*a*	*a*
18	$O_{3'}$	7.4	7.4	6.9	6.8	8.2	8.3
2	$C_{1'}$	20.9	21.1	19.2	19.5	18.9	19.3
4	$C_{4'}$	32.0	30.5	*b*	*b*	*b*	*b*
20	C_2	45.5	45.2	45.9	45.6	46.9	46.8

[a] BLYP and BP86 predict that anion structure **22** collapses to that of anion **16**. [b] BLYP and BP86 predicts that anion structure **4** dissociates.

The energetic order of the anions can be *partially* expressed as

$$\text{N(amino)} < \text{O(hydroxyl)} < \text{C(aliphatic)} < \text{C(aromatic)}$$

with some exceptions that will be considered in the following discussion. Among the radicals produced at the aliphatic carbons, only **1** gives a stable anion. Anion **2**, like radical **1**, has the adenine fragment almost coplanar with respect to the sugar ring, with $\chi = 168°$ (see Figures 2 and 3). Carbon atom $C_{1'}$ has an sp^3 hybridization, and the glycosyl link is longer than in **1** (1.39 Å → 1.44 Å) and similar to the bond length in 2′-dAdo. The two links with the adjacent atoms $C_{2'}$ and $O_{4'}$ increase in length, assuming values similar to the ones found in the neutral 2′-dAdo. The only difference in the dihedral angles is observed for the hydroxyl groups (β and ϵ), probably because they tend to orient toward the negative charged site, allowing for electrostatic interaction to increase. Optimization of anion **2** constraining the χ dihedral angle to the value found for 2′-dAdo ($\chi = -125°$) gives a structure that is 10.5 kcal/mol higher in energy. This compares with the theoretical pairing energy of AT, −13.8 kcal/mol; thus, our model predicts that in anion **2** the adenine moiety will be paired to the thymine base, with a stabilization with respect to the rotated form of less than 4 kcal/mol.

The B3LYP functional predicts for anion **4** a structure that is similar to 2′-dAdo, with an sp^3 hybridized $C_{4'}$ and a very long $C_{5'}-O_{5'}$ bond length, 1.61 Å, compared to 1.43 Å in 2′-dAdo. This is symptomatic of a possible bond break, but the structure may still be considered to be viable. In contrast, with the BLYP and BP86 functionals, heterolytic dissociation of the $C_{5'}-O_{5'}$ bond, leading to the hydroxyl anion (OH^-), is predicted. The picture in this case is thus different depending on the functional. BLYP and BP86 agree that the hydroxyl group formed will abstract a proton from the molecule. However, in BLYP the reaction is with the hydrogen atom linked to $O_{3'}$, while in BP86 the reaction occurs with H_8, which is linked to the purinic carbon C_8. The product of this reaction is a water molecule and the respective anion. Both of these reactions are predicted to be exothermic by more that 60 kcal/mol. In DNA this reaction would be interpreted as a bond break at the $C_{5'}-O_{5'}$ link, forming a phosphate group that in turn corresponds to a single strand break (SSB). In the latter case, it would be

SCHEME 1: Decomposition Reactions of the Aliphatic Radicals 3, 5, and 9

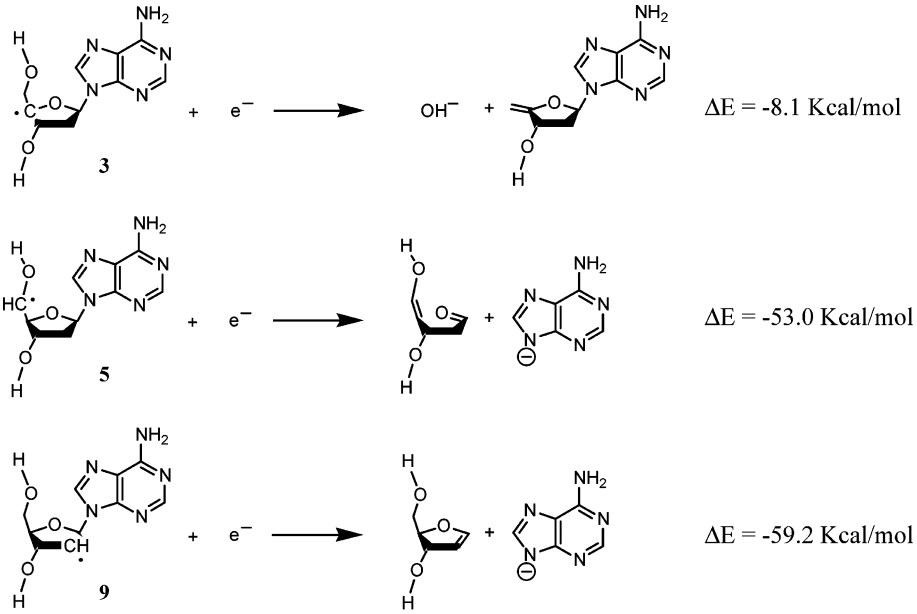

preferable to know the energetics of the bond break without considering the rearrangement reaction. The reaction of radical **3** with an electron, leading to the loss of a hydroxyl group from the $C_{5'}$ position, was considered, and this reaction is also reported in Scheme 1 for clarity:

radical **3** + e^- →
(9-adenosyl)-2-methylene-tetrahydro-furan-3-ol + OH^-

Here, the energy change, ΔE, is found to be slightly *negative*: −8.1 kcal/mol. This indicates that the dissociation reaction is energetically favorable.

Anion **6** is dissociative in nature at the $C_{4'}-O_{4'}$ bond, and this entails an opening of the ribose ring. The glycosyl bond length is increased, going from a value of 1.45 Å in 2′-dAdo to 1.60 Å, this being symptomatic of a possible bond breakage. The dissociation reaction at the N−C glycosyl and the rearrangement of the ribose ring were studied at the B3LYP/DZP++ level (see Scheme 1):

radical **5** + e^- →
9-adenosyl anion + 3,5-dihydroxy-4-pentenal

The energy change is $\Delta E = -53.0$ kcal/mol, demonstrating that the reaction is extremely exothermic. The homolytic cleavage of the glycosidic bond by reduction of radical **5** was found to have a *positive* ΔE, showing that the negative charge is more stable on the adenine moiety with respect to the product of decomposition of the ribose ring (see NPA).

Anion **8** is the only structure that has a $C_{3'}$-*endo* conformation at the ribose ring. The hydrogen connected to $O_{5'}$ migrates to $C_{3'}$, giving simply a different conformer of anion **16**. Dissociation of the glycosyl link is also found for anion **10**. The energetics of the bond break were computed at the B3LYP/DZP++ level of theory (see Scheme 1):

radical **9** + e^- →
9-adenosyl anion + 1,2-didehydro-1,2-dideoxyribose

This reaction is highly exothermic, $\Delta E = -59.2$ kcal/mol.

The anions generated at the oxygen atoms do not show large deviations from the 2′-dAdo geometry. In anion **16**, for example, only the bond lengths near the $O_{5'}$ and $O_{4'}$ sites are affected by formation of the anion (see Figure 5). In anion **16**, the distance $O_{5'}-C_8$ is shorter than for 2′-dAdo, 3.60 Å → 2.87 Å, and this is caused by the interaction of the negatively charged $O_{5'}$ with hydrogen H_8. This anion (**16**) is the lowest lying energetically of those considered in the present study, probably both for the high acidity of the hydroxyl group and the stabilization of the anion by intramolecular interactions. Anion **18**, which is pedagogically created by removal of a hydrogen atom from $O_{3'}$, lies 7 kcal/mol higher in energy, giving us an idea of how strong is the interaction that stabilizes anion **16**, since in the former anion no stabilization from interaction with hydrogen atoms can occur.

The anions generated (qualitatively) at the nitrogen atoms and aromatic carbons have the following relative energetic order:

12 N_{6a} (0.0) < **14** N_{6b} (0.6) < **22** C_8 (3.4) < **20** C_2 (43.6)

These results may be compared to the analogous isolated *adenine* predictions:[29]

12 N_{6a} (0.00) < **14** N_{6b} (0.5) < **22** C_8 (18.3) < **20** C_2 (43.8)

We see that the ribose ring does not affect the energetic ordering and that the only discrepancy is found for anion **18**. This can be easily explained looking at the geometry of anion **18**, in which the carbanion center C_8 interacts with the polarized hydrogen of the $O_{5'}$ hydroxyl group by hydrogen bonding. This has an effect on the $O_{5'}-C_8$ distance, making it shorter than in 2′-dAdo, 3.60 Å → 2.73 Å. Since in the DNA structure the hydroxyl group connected to $C_{5'}$ is replaced by a phosphate group, this stabilizing effect would not affect anion **22**. Thus, in DNA anion **22** will be higher in energy with respect to the most stable anion; in this case, the energy should be intuitively ca. 18 kcal/mol higher with respect to the most stable anion **12**, as in adenine. The BLYP and BP86 functionals both predict that in anion **22** the hydrogen atom $H_{5'}$ will migrate directly to C_8, giving a structure that corresponds to anion **16**.

Large geometrical distortions at the ribose ring are observed for the two anions **12** and **14** created at the amino group (see Figure 4). The ribose ring adopts in both cases an $O_{4'}$-*endo* conformation that corresponds to an "open" structure; the

dihedral angle δ is indicative of this, going from a value of 142° in radical **11** to 106° in anion **12**. This is quite remarkable because the $O_{4'}$-*endo* conformation of the ribose ring is usually considered a potential energy barrier for the interconversion of the $C_{2'}$-*endo* to $C_{3'}$-*endo* and never as a minimum. Inspection of the low vibrational frequencies of anions **12** and **14** showed that they are *real*, thus confirming that the geometries are minima. The $O_{5'}-C_8$ distances are, respectively, 4.74 and 4.72 Å. The amino group hydrogen is coplanar with the adenine plane; this was also found only for the related radicals **11** and **13**. Bond lengths in the adenine framework differ substantially from both the closed-shell neutral 2′-dAdo and radical **11**.

Last in the energetic order is found anion **20** created at the C_2 center, which is in an isolated portion of the molecule, and no interaction with other residues can stabilize the negative charge. The conformation at the ribose ring is $C_{1'}$-*endo*, and the adenine group is rotated with respect to the usual anti form (χ: $-126° \rightarrow 173°$), being almost coplanar with the ribose ring.

The optimized geometries of the stable anions were also used as starting points for geometry optimizations of the respective radicals. In some cases, this led to lower energy minima (**2**, **16**, and **22**). These show minor rearrangements in the structures with respect to the original radicals (**1**, **15**, and **21**) caused by the interaction of the two hydroxyl groups with the adenine moiety. For example, the largest energy stabilization is observed for the radical optimized from anion **22**, with the energy difference with respect to radical **21** being very small, 0.09 eV (2 kcal/mol). Optimization of the radicals starting from the geometry of anions **4** and **22** led to structures that are identical to those of the respective radicals **3** and **17**. The third case is represented by anions **12**, **14**, and **20**, for which the optimization process results in structures that are very slightly higher in energy (ca. 0.01 eV) than the original radicals **11**, **13**, and **19**. Therefore, for these radicals there is a local minimum in the neighbor of the respective anion minimum that is higher in energy than the minima in which radicals **11**, **13**, and **19** sit. This is possible since the anions have very distorted geometries and we are comparing portions of conformational space that are far away. In this case it is very likely that there would be more than one local minimum along the path that connects the two different portions of space; thus, the optimization algorithm can stop in one of the many minima without reaching the minimum that was obtained starting from the 2′-dAdo structure. These results confirm the hypothesis of the complexity of the conformational space and show that there is no guarantee that the structures we have studied are *global* minima in the conformational spaces. However, the results for the energetics show that the different conformations are very near in energy, in a range of at most a few kcal/mol. This result also implies that all the properties computed as the difference of anion and radical energies should be understood as local.

3.2. Adiabatic Electron Affinities, Vertical Electron Affinities, and Vertical Detachment Energies. The adiabatic electron affinities were computed with the three different functionals for those anions that are stable. In Table 3 we report the values computed with and without harmonic zero point vibrational corrections. This correction has little effect on the relative energies; the variation is generally less that 0.15 eV. The values are found to be large and spread over a range of 0.99−3.47 eV.

Comparison can be made with the previously determined AEAs of the radicals generated from isolated *adenine*:[29] AEA(**11** N_{6a}) = 2.55 eV, AEA(**13** N_{6b}) = 2.58 eV, AEA(**19** C_2) = 0.90 eV, AEA(**21** C_8) = 2.38 eV. The relative order is different for the radicals derived from 2′-dAdo. This difference is most clearly represented by **21**, which has the highest AEA: 3.14 eV (B3LYP). This is rationalized by the fact that the energy stabilization derived from the interaction with the ribose ring residues can affect only anion **22**, as was already noticed in the previous section.

TABLE 3: Adiabatic Electron Affinities (eV) of the Radicals Derived from Adenosine, with ZPVE Corrected Values in Parentheses

structure		B3LYP	BLYP	BP86
1	$C_{1'}$	1.33	1.33	1.53
		(1.36)	(1.36)	(1.56)
3	$C_{4'}$	0.94	*a*	*a*
		(1.03)	*a*	*a*
11	N_{6a}	2.65	2.55	2.78
		(2.65)	(2.56)	(2.78)
13	N_{6b}	2.66	2.57	2.80
		(2.66)	(2.57)	(2.80)
15	$O_{5'}$	2.77	2.62	2.84
		(2.79)	(2.66)	(2.88)
17	$O_{3'}$	2.43	2.40	2.58
		(2.47)	(2.44)	(2.62)
19	C_2	1.03	0.99	1.14
		(1.10)	(1.07)	(1.22)
21	C_8	3.14	3.30	3.40
		(3.19)	(3.34)	(3.47)

[a] BLYP and BP86 predict that anion **4** is not stable.

TABLE 4: Vertical Electron Affinities (eV) of the Radicals Derived from Adenosine

structure		B3LYP	BLYP	BP86
1	$C_{1'}$	0.19	0.36	0.46
3	$C_{4'}$	0.35	0.59	0.69
5	$C_{5'}$	0.08	0.33	0.44
7	$C_{3'}$	0.08	0.34	0.44
9	$C_{2'}$	1.02	1.12	1.26
11	N_{6a}	2.27	2.17	2.39
13	N_{6b}	2.29	2.20	2.42
15	$O_{5'}$	2.41	2.24	2.44
17	$O_{3'}$	2.16	2.13	2.29
19	C_2	0.14	0.33	0.44
21	C_8	1.71	1.69	2.15

Radicals **1** and **3**, generated on the aliphatic carbons, show smaller AEAs, because of the general tendency of aliphatic carbon atoms to poorly handle negative charges in the sp^3 orbitals. For comparison, the CH_3 radical has an AEA of less than 0.1 eV.

Radicals **15** and **17**, produced by removing a hydrogen atom from the oxygen atoms, have high AEAs (2.77 and 2.43 eV, with B3LYP), and this is quite easily understood since the oxygen atom has a high tendency to accommodate a negative charge.

The vertical electron affinities are reported in Table 4. These results give insight to understanding the role of geometrical rearrangement in the stabilization of the anions and the energy release from the near-instantaneous addition of an electron to the radicals. Further, these findings make possible a simple analysis of the unstable anions that were not taken into consideration in the AEA computations. The fact that the VEAs are lower than the AEAs for all species is symptomatic of the fixed geometrical rearrangement of the anion nuclei and the simultaneous relaxation of the electronic density.

In all cases, the VEAs were found to be *positive*. For the aliphatic radicals the values are almost zero (0.08 eV for **5** and **7**), and the nature of the transient anions (bound or unbound) remains uncertain because of the ±0.12 eV error bracket of the method used.[50] We conclude that geometrical rearrangement

TABLE 5: Vertical Detachment Energies (eV) of the Anions Derived from Adenosine

structure		B3LYP	BLYP	BP86
2	$C_{1'}$	2.07	1.94	2.17
4	$C_{4'}$	1.78	*a*	*a*
12	N_{6a}	2.80	2.67	2.90
14	N_{6b}	2.82	2.69	2.92
16	$O_{5'}$	3.17	2.92	3.16
18	$O_{3'}$	2.67	2.66	2.85
20	C_2	1.92	1.84	1.99
22	C_8	3.65	2.92	3.16

[a] BLYP and BP86 predict that anion **4** dissociates; see text.

plays a key role in stabilizing anions **2** and **4**. An exception among carbon radicals is presented by radical **9** ($C_{2'}$) with a VEA equal to 1.02 eV (B3LYP).

Radicals produced on heteroatoms (**11**, **13**, **15**, and **17**) have high VEA (>2 eV), confirming that the values of these AEAs are caused by the intrinsic tendency of those atoms to accept an excess of negative charge, with little contribution to the AEAs caused by geometrical rearrangements.

The same analysis applied to the aromatic radicals **19** and **21** leads us to the conclusion that for **19** (C_2) the geometrical perturbation is the major contribution to the stability of anion **20**. The geometrical rearrangement also contributes substantially in the AEA of radical **21** (3.14 eV), since the VEA was found to be much smaller (1.71 eV).

The vertical detachment energies (VDEs) are listed in Table 5. Large VDEs are found for all the anions considered, with the smallest one being found for anion **4** (1.78 eV). This quantity may be interpreted in an inverse manner with respect to the VEA, namely, comparison with the AEAs can tell us how important is the geometrical relaxation of the fixed nuclei in the transition to the radical from the anion. Significant differences between the VDEs and the AEAs (>1 eV) are found for anions **2**, **4**, and **20**. For the other anions, which are created at heteroatoms, there is little difference between the VDEs and AEAs. Here the same conclusion on the importance of geometry relaxation of the fixed nuclei applies to the radicals. As pointed out above, an experimental investigation of the anions based on photoelectron spectroscopy would be able to identify only 7 of the 11 anions studied due to the instability of 4 of the aliphatic carbanions.

3.3. Spin Distributions, Nature of the Anions, and Atomic Charges. The unpaired spin densities of the radicals computed with a contour value of 0.001 au are depicted in Figure 6. The five aliphatic radicals (**1**, **3**, **5**, **7**, and **9**) and the two oxygen atom radicals (**15** and **17**) display p orbital-like spin distributions at the radical centers. In **1** the unpaired electron is partially delocalized on the adenine five membered ring.

In the other six radicals generated on the ribose ring, the bulk of the spin density is found near the radical center and is limited to the ribose ring only. Radicals **3**, **5**, and **7** show π conjugation with an oxygen atom in the α position, respectively $O_{4'}$, $O_{5'}$, and $O_{3'}$, thus confirming that the higher stability of those radicals with respect to **9** has its origin in the proximity of one oxygen atom. The nitrogen radicals **11** and **13** have typical π shaped spin densities, which are almost entirely restricted to the adenine framework. The highest energy radicals **19** and **21** are characterized by the shape of a lone pair protruding from the radical center. Some delocalization effects are observed and may be interpreted as hyperconjugation, since the symmetry of the spin density is not compatible with that of a p orbital conjugated system.

Examination of the HOMOs of all the anions leads us to the expected conclusion that these species have covalent bound

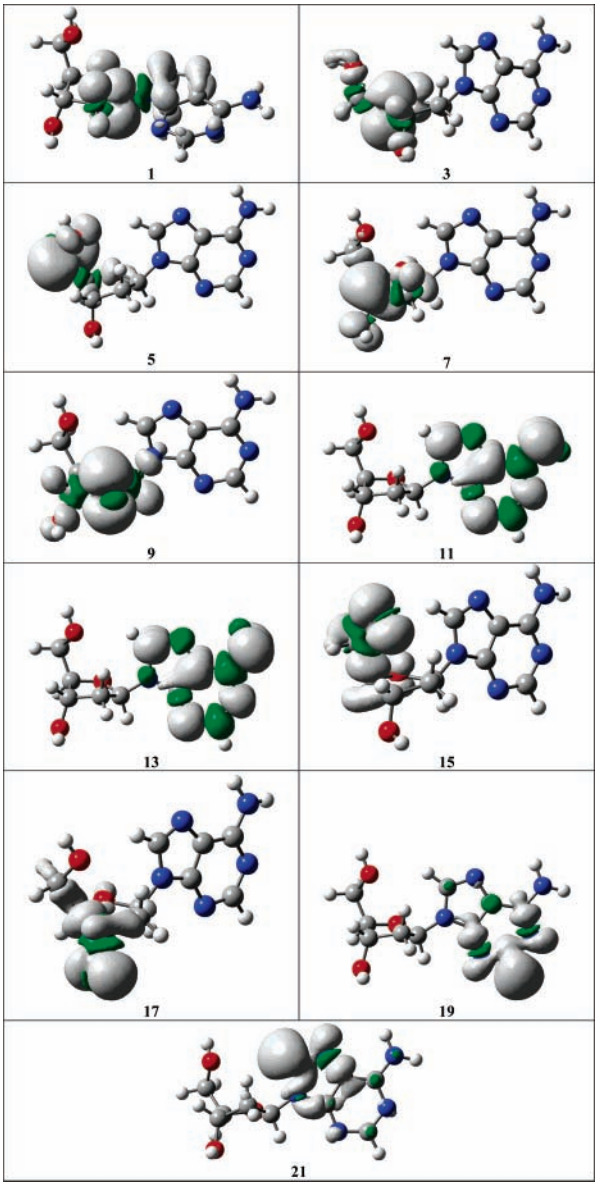

Figure 6. Spin density of the radicals predicted at the B3LYP/DZP++ level of theory.

character. The same conclusion was drawn for the isolated closed-shell adenine anions.[29] This finding is also supported by the fact that the anions are closed-shell species and, as noted in the geometry section, significant geometrical relaxation is observed. The HOMO of anion **4** shows an antibonding character at the $C_{5'}-O_{5'}$ link, confirming the suspected dissociative character of this anion showed by the BLYP and BP86 functionals.

The Weinhold natural population analysis (NPA) charges were computed. In Table 6 we report the total charge on the ribose and on the adenine fragments for both the radicals and the anions. We also computed the difference between the radical and the anion charges to elucidate how the excess charge is redistributed between the two species following anion formation. The charge distributions for the neutral radicals are almost identical for all the species. The polarization of the electrons is such that for radicals the ribose ring is always found positively charged in the range 0.26−0.32. Richardson[38] found that for each of the four neutral 2′-deoxyribonucleosides found in DNA the charge division is the same, with the sum of NPA equal to 0.31 for the ribose.

TABLE 6: Natural Population Analysis (NPA) Charges of the Radicals and Anions Derived from Adenosine (DZP++ B3LYP Method)

radicals			anions			Δq^a	
structure	ribose	adenine	structure	ribose	adenine	ribose	adenine
1 $C_{1'}$	0.32	−0.32	2 $C_{1'}$	−0.45	−0.55	0.77	0.23
3 $C_{4'}$	0.26	−0.26	4 $C_{4'}$	−0.63	−0.37	0.89	0.11
5 $C_{5'}$	0.29	−0.29	6 $C_{5'}$	−0.52	−0.48	0.81	0.19
7 $C_{3'}$	0.29	−0.29	8 $C_{3'}$	−0.61	−0.39	0.90	0.10
9 $C_{2'}$	0.28	−0.28	10 $C_{2'}$	−0.10	−0.90	0.38	0.62
11 N_{6a}	0.30	−0.30	12 N_{6a}	0.20	−1.20	0.10	0.90
13 N_{6b}	0.30	−0.30	14 N_{6b}	0.21	−1.21	0.09	0.91
15 $O_{5'}$	0.27	−0.27	16 $O_{5'}$	−0.63	−0.37	0.90	0.10
17 $O_{3'}$	0.27	−0.27	18 $O_{3'}$	−0.64	−0.36	0.91	0.09
19 C_2	0.29	−0.29	20 C_2	0.24	−1.24	0.05	0.95
21 C_8	0.29	−0.29	22 C_8	0.03	−1.03	0.26	0.74

[a] Δq is the difference between the radical and anion charges for each fragment, $\Delta q(\text{fragment}) = q_{\text{rad}}(\text{fragment}) - q_{\text{an}}(\text{fragment})$.

The radical that has the ribose most positively charged is $C_{1'}$. Again, this confirms the delocalization of the unpaired electron on the adenine fragment.

It is interesting to ask how the anion's "last" electron will be distributed in the molecule. Examining the last two columns of Table 6, we find that the charge goes, as intuitively expected, mostly to the site where the hole was created. For the stable ribose ring radicals, we find that the sum of NPA charges on ribose is smaller for the aliphatic carbon radicals (0.77 and 0.89 for **2** and **4**, respectively) and higher for the oxygen atom radicals (0.90 for **15**). Anions **6** and **10** are dissociated species. Anion **6** follows the general trend, with the "last" electron being mostly on the ribose ring (0.81), but when dissociated at the glycosyl link, we find that the negative charge is more stable on the adenine fragment (this was confirmed by computations of the energetics). Anion **10** also displays this feature; in the optimized structure most of the charge is on the adenine structure (0.62). In the anions produced on the adenine framework, the charge is mostly on the purine ring. Radical **21** has the lowest Δq (0.74) for the adenine fragment. Again, a look at the geometry helps us understand the reason for this result. The interaction of C_8 with $H_{5'}$ polarizes the negative charge, and this is confirmed by the NPA, which indicates that a fraction of the charge is accommodated on $H_{5'}$ and $O_{5'}$ atoms ($\Delta q_H = 0.06$ and $\Delta q_O = 0.08$).

4. Biological Implications

From the results reported in the previous section we draw the following picture, described visually by Scheme 2. We start from a primary event capable of abstracting one hydrogen atom from the B DNA structure. This could be a chemical reaction with some reactive species such as the hydroxyl radical ($OH^{\bullet}$).[2−4] The abstraction reaction

$$R^{\bullet} + MH \rightarrow RH + M^{\bullet}$$

is possible only for those hydrogen atoms that can be reached by the reactants. The relative cross section for this reaction may be intuitively factorized in two terms, one relative to the activation barrier energetics (k, a rate constant) and a statistical factor connected to the area available for the abstraction (A, accessibility area):

$$\sigma_{\text{rel}} \sim k_{\text{rel}} A_{\text{rel}}$$

The relative rate constant k_{rel} has been associated with the bond strength by the empirical formula[30]

$$k^{\text{rel}} = e^{-0.5\Delta\Delta E_{C-H}}$$

where $\Delta\Delta E_{C-H}$ is the energy difference between two bond strengths. The values of the relative rate constant (k_{rel}) predicted for the 2′-dAdo *aliphatic* radicals are

$$C_{1'}\,(\mathbf{1}) = 1.00, \quad C_{4'}\,(\mathbf{3}) = 0.36, \quad C_{5'}\,(\mathbf{5}) = 0.15,$$
$$C_{3'}\,(\mathbf{7}) = 0.11, \quad C_{2'}\,(\mathbf{9}) = 0.01$$

The other radicals, respectively the ones produced at the heteroatoms and at the aromatic carbons, are much higher in energy, and thus, the relative rate constant for homolytic bond break is virtually zero.

In the B DNA form, the 5′ and 4′ positions are accessible from the minor groove, and a small molecule such as the hydroxyl radical can reach those two positions. The 2′ position

SCHEME 2: Predicted Fate of the Adenosine Radicals Generated from DNA

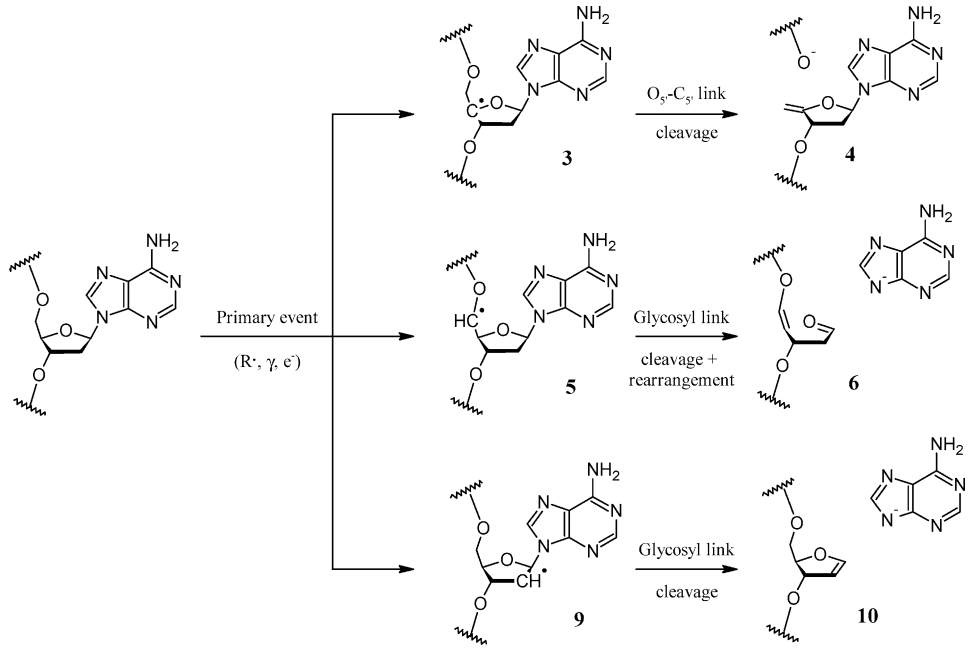

is accessible, on the contrary, from the major grove. This site is not considered to be an important abstraction site, probably due to both the low accessibility and the low reactivity.[4] The relative accessibilities of hydrogens (A_{rel}) in B-DNA are[30,59]

$$C_{1'}(\mathbf{1}) = 0.00, \quad C_{4'}(\mathbf{3}) = 0.44, \quad C_{5'}(\mathbf{5}) = 1.00,$$
$$C_{3'}(\mathbf{7}) = 0.19, \quad C_{2'}(\mathbf{9}) = 0.11$$

Combining these two theoretical results, we evaluated the relative cross sections (σ_{rel}). The highest values were found for the following sites:

$$C_{4'}(\mathbf{3}) = 1.00 \approx C_{5'}(\mathbf{5}) = 0.95 > C_{3'}(\mathbf{7}) = 0.13 >$$
$$C_{2'}(\mathbf{9}) = 0.01 > C_{1'}(\mathbf{1}) = 0.00$$

Investigation conducted on a model of 2′-deoxyribose at the MP2/6-31G* level of theory gave the following relative cross sections for the 1′−4′ sites, in accord with our findings:

$$C_{4'}(\mathbf{3}) = 1.00 > C_{3'}(\mathbf{7}) = 0.73 > C_{2'}(\mathbf{9}) = 0.06 >$$
$$C_{1'}(\mathbf{1}) = 0.00$$

These results imply that the highly exposed (high A_{rel}) and high reactive (high k_{rel}) hydrogen atoms linked to $C_{4'}$ and $C_{5'}$ are the most important sites for radical formation when the radical is generated from another radical. This result may be extended to the other three nucleosides supposing that the influence of a different base (T, G, or C) would not affect the *aliphatic* carbon radicals' energetic order. The interaction with highly energetic photons (γ-ray, UV) also affects DNA in many ways. One is direct interaction with the nucleotides, giving dissociative excited states or photoionization of the nucleotides followed by deprotonation, that is

$$h\nu + MH \rightarrow (MH)^{\bullet +} + e^- \rightarrow M^{\bullet} + H^+ + e^-$$

A second possibility is generation of radicals from the molecular environment (for example $OH^{\bullet}$ from water) that can in turn abstract a hydrogen atom from the nucleotides.[8]

The reaction of DNA components with electrons has recently gained much attention.[11−14,21,60−62] Different mechanisms are considered to be relevant depending on the energy of the electrons. Two energetic ranges are typically considered by experimentalists, low ($E < 15$ eV) and high ($E \sim 15-100$ eV).

At low energy, resonant mechanisms are thought to predominate. For example, dissociative electron attachment can lead to the formation of radicals and a hydride anion,

$$e^- + MH \rightarrow (MH)^{*-} \rightarrow M^{\bullet} + H^-$$

Another possible mechanism for radical formation is electron autodetachment from the transient molecular anion, $(MH)^{*-}$. This event may lead to an excited electronic state that is dissociative in nature and can undergo homolytic bond breakage at one bond

$$e^- + MH \rightarrow (MH)^{*-} \rightarrow (MH)^* + e^- \rightarrow M^{\bullet} + H^{\bullet} + e^-$$

At high energies, nonresonant mechanisms such as inelastic scattering of electrons may lead to the formation of a neutral excited electronic state that may have many dissociative channels leading to both homolytic and heterolytic bond breaking,

$$(MH)^* \rightarrow M^{\bullet} + H^{\bullet}, M^+ + H^-, M^- + H^+, \text{etc.}$$

High energy electrons may also induce ionization reactions leading to either the ground state or an excited electronic state of a cation

$$e^- + MH \rightarrow (MH)^+ + 2e^-, (MH)^{*+} + 2e^-$$

This cation may in turn experience different dissociation paths producing both radicals and cations

$$(MH)^{*+}, (MH)^+ \rightarrow M^{\bullet} + H^+, M^+ + H^{\bullet}$$

Once one of the radicals is produced, there are two possible ensuing paths. The first can be the reaction of the radical with one DNA residue, reaction with some other species, or a repair reaction. The second path entails the binding of one electron to form an anion and represents the second step toward the damage of the DNA double strand. This reaction competes with the first path and can be initiated only by an electron produced from the primary event, for example, the radiolysis of a water molecule,[63] or by a reducing species.

The nature of the radical will determine the anion produced and the possible damage. According to the present research, there are three radical sites in the 2′-dAdo molecule that, once reduced, can generate damage to the DNA double strand: $C_{4'}$ (**3**), $C_{5'}$ (**5**), and $C_{2'}$ (**9**). All those lead to an SSB. Anion **4** has a dissociative nature with respect to the $O_{5'}-C_{5'}$ link, a process that is followed by rearrangement at $C_{5'}$ to form a methylene group. The fragment obtained from dissociation of anion **4** is itself also very reactive and can undergo hydrolysis of the enol ether group to form an opened ribose ring (see Scheme 1 for the structure). Anions **6** and **10** both lead to dissociation of the $C_{1'}-N_9$ glycosyl link, giving the 9-adenosyl anion, a rearranged opened ring, and a closed ribose ring, both containing an enol ether group that may be hydrolyzed (Scheme 1). From the energetic point of view, the three radicals that lead to damage have high stability with respect to the other possible radicals [1.9 (**3**), 3.9 (**5**), and 8.7 (**9**) kcal/mol with respect to **1**], leading to the conclusion that they can be formed easily. As we have pointed out before, steric effects reduce the probability of producing radical **9** when the primary event is caused by a radical.

Experimental evidence for the dissociative nature of anions **4** and **10** may be found in the results of the low-energy collision-induced dissociation experiments of Rodgers et al.[64] These were interpreted using a mechanism that involves an initial proton transfer from the rybosil group to the phosphate anion to form anions at the ribose ring. Two major deprotonation sites were found, the 2′ and the 5′ positions on the ribose ring, that correspond in our case to the anions obtained from radicals **3** and **9**. The dissociation products derived from the unstable anions correspond to those predicted for the 2′-dAdo anions (Scheme 1).

The formation of 5′,8-cyclo-2′-deoxy-7-adenosil radical from radical **5** can be one of the processes competing with the reduction of **5**. This reaction was studied in the 2′-dAdo molecule by Chatgilialoglu et al.,[6] who do not mention the reduction pathway, probably because cyclization is predominant with respect to it.[6] The measured rate constant for the cyclization reaction of **5** is of the order of 10^5 s^{-1}. The authors[6] also expect that in DNA the rate constant will decrease considerably due to both enthalpic and entropic effects. It is important to observe that the geometrical rearrangement that leads to this molecular species might have a high transition state energy in DNA, because of the geometrical constraints that are found in the double strand and which do not exist in the model molecule

2′-dAdo. On the contrary, the three radicals **3**, **5**, and **9** produce dissociative potential energy surfaces in the anionic states, and no transition state has to be climbed to reach the final structures. The effect of this may be that in DNA the ratio of the reaction rates for the rearrangement and the reduction step will see the reduction path favored.

Even if this discussion is centered on the radical chemistry, we stress the fact that the damage produced because of the dissociative nature of the anions can occur *directly* if there is a path leading from the neutral structure to the closed-shell anions. The recent studies on highly energetic electrons[11−14] have suggested that production of excited molecular states can lead to heterolytic dissociation, with this representing a direct mechanism for anion formation.

We expect to find a similar behavior in DNA, thus predicting that the abstraction−reduction path and direct formation of the anions could be an important cause of strand breaks. Further investigation of the nucleotides is required to elucidate this point, since in our case we are not considering the effect of the phosphate group.

5. Conclusions

The radicals and the anions produced from the adenosine molecule by removal of one of the hydrogen atoms were investigated using a carefully calibrated method based on density functional theory. The combination of functional and basis set used is capable of predicting adiabatic electron affinities with an average error less than 0.12 eV.[50]

From the present study, we draw the following conclusions:

1. The radicals produced show modest geometrical relaxation with respect to the 2′-dAdo geometry, mainly caused in the aliphatic radicals by planarization at the carbon center. Radical **1** ($C_{1'}$) shows rotation of the adenine moiety along the glycosyl link with a stabilization of ca. 4 kcal/mol. The aliphatic radicals were found to be the most stable, with the following ordering:

$$1' (\mathbf{1}) > 4' (\mathbf{3}) > 5' (\mathbf{5}) > 3' (\mathbf{7}) > 2' (\mathbf{9})$$

with radical **1** being the lowest in energy, since it is stabilized by conjugation with the purinic ring. The stability order with respect to the other radicals is

$$\text{C(aliphatic)} < \text{N(amino)} < \text{O(hydroxyl)} < \text{C(aromatic)}$$

2. The only stable *aliphatic* anion is the one produced at $C_{1'}$, which has the adenine moiety rotated as in radical **1**. The other *aliphatic* anions undergo dissociation of one or more bonds (**4**, **6**, and **10**) or hydrogen migration (**8**). The anions produced on the adenine framework show rearrangement of the ribose ring to an $O_{4'}$-*endo* (**12** and **14**) or rotation of the adenine framework along the glycosidic bond (**20**). The rationalized anion energetic order follows the trend

$$\text{N(amino)} < \text{O(hydroxyl)} < \text{C(aliphatic)} < \text{C(aromatic)}$$

3. The AEAs were computed for the stable anions, and the values are found to be positive and large, in the range 0.99−3.47 eV. Analysis of the vertical electron affinities shows that in aliphatic anions this energy difference is small and that geometry relaxation gives the major contribution to the AEAs. The radicals created at heteroatoms have high VEAs due to the intrinsic capacity of the heteroatoms to accommodate extra negative charge.

4. The spin density of the aliphatic carbon radicals is usually localized at the center where the radical is produced. A delocalized spin density is found for **1** ($C_{1'}$) and for the nitrogen radicals **11** and **13**. The closed-shell anion HOMOs are found to have the expected covalent nature for all species considered.

5. The biological implication of the instability of anions **4**, **6**, and **10** is the generation of single strand breaks of DNA. The radicals that lead to these anions are more easily formed for both energetic and steric reasons. Reduction of radical **3** gives a bond break at the $O_{5'}-C_{5'}$ link, while radicals **5** and **9** lose the base under the form of the 9-adenosyl anion. The reduction step, competing with other mechanisms, such as internal rearrangement (mainly cyclization), reaction with other reactive species, and repair reactions, determines the extent of this type of damage.

Acknowledgment. This research was supported by the U.S. National Science Foundation, Grant CHE-0136186. The authors thank Dr. Nancy Richardson for several helpful discussions in the early phase of the project. F.A.E. thanks L. Blissett and F. Fiché-Amat for insightful discussions.

Supporting Information Available: Tables giving total energies of the radicals derived from adenosine and of the stable anions derived from adenosine radicals. This material is available free of charge via the Internet at http://pubs.acs.org.

References and Notes

(1) Cleaver, J. E. *DNA Repair* **2002**, *1*, 977.
(2) Steenken, S. *Chem. Rev.* **1989**, *89*, 503.
(3) Vieira, A. J. S. C.; Steenken, S. *J. Am. Chem. Soc.* **1990**, *112*, 6986.
(4) Pogozelski, W. K.; Tullius, T. D. *Chem. Rev.* **1998**, *98*, 1089.
(5) Flyunt, R.; Bazzanini, R.; Chatgilialoglu, C.; Mulazzani, Q. G. *J. Am. Chem. Soc.* **2000**, *122*, 4225.
(6) Chatgilialoglu, C.; Guerra, M.; Mulazzani, Q. G. *J. Am. Chem. Soc.* **2003**, *125*, 3839.
(7) Ramírez-Arizmendi, L. E.; Heidbrink, J. L.; Guler, L. P.; Kenttämaa, H. I. *J. Am. Chem. Soc.* **2003**, *125*, 2272.
(8) Close, D. M. *Radiat. Res.* **1993**, *135*, 1.
(9) Steenken S.; Goldbergerova, L. *J. Am. Chem. Soc.* **1998**, *120*, 3928.
(10) Douki, T.; Angelov, D.; Cadet, J. *J. Am. Chem. Soc.* **2001**, *123*, 11360.
(11) Huels, M. A.; Hahndorf, I.; Illenberger, E.; Sanche, L. *J. Chem. Phys.* **1998**, *108*, 1309.
(12) Abdoul-Carime, H.; Cloutier, P.; Sanche, L. *Radiat. Res.* **2001**, *155*, 625.
(13) Abdoul-Carime, H.; Sanche, L. *Int. J. Radiat. Biol.* **2002**, *78*, 89.
(14) Huels, M. A.; Boudaïffa, B.; Cloutier, P. Hunting, D.; Sanche, L. *J. Am. Chem. Soc.* **2003**, *125*, 4467.
(15) Wiley, J. R.; Robinson, J. M.; Ehdaie, S.; Chen, E. C. M.; Chen, E. S. D.; Wentworth, W. E. *Biochem. Biophys. Res. Commun.* **1991**, *180*, 841.
(16) Sharma, S.; Lee, J. K. *J. Org. Chem.* **2002**, *67*, 8360.
(17) Chandra, A. K.; Nguyen, M. T.; Uchimaru, T.; Zeegers-Huyskens, T. *J. Phys. Chem. A* **1999**, *103*, 8853.
(18) Desfrançois, C.; Abdoul-Carime, H.; Schermann, J. P. *J. Chem. Phys.* **1996**, *104*, 7792.
(19) Schiedt, J.; Weinkauf, R.; Neumark, D. M.; Schalg, E. W. *Chem. Phys.* **1998**, *239*, 511.
(20) Periquet, V.; Moreau, A.; Carles, S.; Sherman, J. P.; Desfrançois, C. *J. Electron Spectrosc. Relat. Phenom.* **2000**, *106*, 141.
(21) Gohlke, S.; Abdoul-Carime, H.; Illenberger, E. *Chem. Phys. Lett.* **2003**, *380*, 595.
(22) Colson, A.; Besler, B.; Close, D. M.; Sevilla, M. D. *J. Phys. Chem.* **1992**, *96*, 661.
(23) Wesolowski, S. S.; Leininger, M. L.; Pentchev, P. N.; Schaefer, H. F. *J. Am. Chem. Soc.* **2001**, *123*, 4023.
(24) Walch, S. P. *Chem. Phys. Lett.* **2003**, *374*, 496.
(25) Richardson, N. A.; Wesolowski, S. S.; Schaefer, H. F. *J. Phys. Chem. B* **2003**, *107*, 848.
(26) Chen, E. S.; Chen, E. C. M. *Biochem. Biophys. Res. Commun.* **2001**, *289*, 421.
(27) Wetmore, S. D.; Boyd, R. J.; Eriksson, L. A. *J. Phys. Chem. B* **1998**, *102*, 10602.
(28) Chen, E. S. D.; Chen, E. C. M.; Sane, N. *Biochem. Biophys. Res. Commun.* **1998**, *246*, 228.
(29) Evangelista, F. A.; Paul, A.; Schaefer, H. F. *J. Phys. Chem. A* **2004**, *108*, 3565.

(30) Miaskiewicz, K.; Osman, R. *J. Am. Chem. Soc.* **1994**, *116*, 232.
(31) Colson, A. O.; Sevilla, M. D. *J. Phys. Chem.* **1995**, *99*, 3867.
(32) Luo, N.; Litvin, A.; Osman, R. *J. Phys. Chem. A* **1999**, *103*, 592.
(33) Brameld, K. A.; Goddard, W. A. *J. Am. Chem. Soc.* **1999**, *121*, 985.
(34) Watson, D. G.; Sutor, D. J.; Tollin, P. *Acta Crystallogr.* **1965**, *19*, 111.
(35) Swaminatha Reddy, B.; Viswamitra, M. A. *Acta Crystallogr.* **1975**, *B31*, 19.
(36) Rozenberg, M.; Jung, C.; Shoham, G. *Phys. Chem. Chem. Phys.* **2003**, *5*, 1533.
(37) Gidden, J.; Bowers, M. T. *J. Phys. Chem. B* **2003**, *107*, 12829.
(38) Richardson, N. A.; Gu, J.; Wang, S.; Xie, Y.; Schaefer, H. F. *J. Am. Chem. Soc*, in press.
(39) Saenger, W. *Principles of Nucleic Acid Structure*; Springer-Verlag: New York, 1984.
(40) Harris, D. G.; Shao, J.; Anderson, J. M.; Marx, D. P.; Zimmerman, S. S. *Nuclosides Nucleotides* **2002**, *21*, 803.
(41) Ghosh, A.; Bansal M. *Acta Crystallogr.* **2003**, *D59*, 620.
(42) Becke, A. D. *J. Chem. Phys.* **1993**, *98*, 5648.
(43) Becke, A. D. *Phys. Rev. A* **1988**, *38*, 3098.
(44) Lee, C.; Yang, W.; Parr, R. G. *Phys. Rev. B* **1988**, *37*, 785.
(45) Perdew, J. P. *Phys. Rev. B* **1986**, *33*, 8822.
(46) Perdew, J. P. *Phys. Rev. B* **1986**, *34*, 7406.
(47) Huzinaga, S. *J. Chem. Phys.* **1965**, *42*, 1293.
(48) Dunning, T. H. *J. Chem. Phys.* **1970**, *53*, 2823.
(49) Lee, T. J.; Schaefer, H. F. *J. Chem. Phys.* **1985**, *83*, 1784.
(50) Rienstra-Kiracofe, J. C.; Tschumper, G. S.; Schaefer, H. F.; Nandi, S.; Ellison, G. B. *Chem. Rev.* **2002**, *102*, 231.
(51) Frisch, M. J.; Trucks, G. W.; Schlegel, H. B.; Gill, P. M. W.; Johnson, B. G.; Robb, M. A.; Cheeseman, J. R.; Keith, T.; Petersson, G. A.; Montgomery, J. A.; Raghavachari, K.; Al-Laham, M. A.; Zakrzewski, V. G.; Ortiz, J. V.; Foresman, J. B.; Cioslowski, J.; Stefanov, B. B.; Nanayakkara, A.; Challacombe, M.; Peng, C. Y.; Ayala, P. Y.; Chen, W.; Wong, M. W.; Andres, J. L.; Replogle, E. S.; Gomperts, R.; Martin, R. L.; Fox, D. J.; Binkley, J. S.; Defrees, D. J.; Baker, J.; Stewart, J. P.; Head-Gordon, M.; Gonzalez, C.; Pople, J. A. *Gaussian 94*, Revision E.2; Gaussian, Inc.: Pittsburgh, PA, 1995.
(52) Reed, A. E.; Weinstock, R. B.; Weinhold, F. *J. Chem. Phys.* **1985**, *83*, 735.
(53) Reed, A. E.; Weinhold, F. *J. Chem. Phys*. **1985**, *83*, 1736.
(54) Reed, A. E.; Curtiss, L. A.; Weinhold, F. *Chem. Rev.* **1988**, *88*, 899.
(55) Reed, A. E.; Schleyer, P. R. *J. Am. Chem. Soc.* **1990**, *112*, 1434.
(56) Sasisekharan, V.; Pattabiraman, N. *Nature* **1978**, *275*, 159.
(57) Toure, P.; Villena, F.; Melikyan, G. G. *Org. Lett.* **2002**, *4*, 3989.
(58) Yanson, I. K.; Teplitsky, A. B.; Sukhodub, L. F. *Biopolymers* **1979**, *18*, 1149.
(59) Sy, D.; Savoye, C.; Begusova, M.; Michalik, V.; Charlier, M.; Spotheim-Maurizot, M. *Int. J. Radiat. Biol.* **1997**, *72*, 147.
(60) Li, X.; Sevilla, M. D.; Sanche, L. *J. Am. Chem. Soc.* **2003**, *125*, 13668.
(61) Barrios, R.; Skurski, P.; Simons, J. *J. Phys. Chem. B* **2002**, *106*, 7991.
(62) Zhao, M.; Xia, Y.; Ma, Y.; Ying M.; Liu, X.; Mei, L. *Phys. Lett. A* **2002**, *300*, 421.
(63) Zhan, C.-G.; Dixon, D. A. *J. Phys. Chem. B* **2003**, *107*, 4403.
(64) Rodgers, M. T.; Campbell, S.; Marzluff, E. M.; Beauchamp, J. L. *Int. J. Mass Spectrom. Ion Processes* **1994**, *137*, 121.